

A FAST ALGORITHM FOR DISPLACEMENT-DRIVEN ELASTIC CONTACT MODELING

GRADINARU Dorin, SPINU Sergiu

University "Stefan cel Mare" of Suceava, ROMANIA

gradinaru@fim.usv.ro, sergiu.spinu@fim.usv.ro

Keywords: elastic contact, numerical simulation, iteration, displacement-driven, conjugate gradient

Abstract: A variation of elastic contact problem is approached in this paper, considering the case when the loading is not known, but the normal displacement is. The algorithm for modeling the classical load-driven elastic contact problem is modified to allow for the new input. Interference equation in the original algorithm is completed with the rigid-body displacement, and pressure correction instruction is removed. Guess values for load and initial pressure are required for iteration of pressure distribution and contact area. Predictions of the numerical program newly advanced are compared with analytical results, for three types of technologically important, axisymmetric contacts, and a good agreement is found.

1. INTRODUCTION

When force is transmitted through a contact between two bodies, assessment of contact area and pressure distribution can provide valuable information concerning the strength of the contact. Stress state induced in subsurface by surface tractions is responsible for plastic yielding and finally for contact failure. With analytical solutions lacking the mathematical support for solving the complex equations which arise (Lamé), numerical approaches have found great applicability to various situations of contact geometry or material response. Great efforts were conducted lately towards increasing the computational efficiency of these methods, as the currently available computational power is easily surpassed by the complexity of the models to be solved. The search for refined numerical methods capable of handling fine meshes and complex patterns of material behavior remains one of the major challenges to be met.

While most algorithms are centered on the load-driven formulation, the displacement-driven elastic contact problem has received little attention. Boucly, Nélias and Green, [1], have included a displacement driven elastic contact solver in their elastic-plastic contact algorithm. Gallego, [3], advanced an extended elastic contact solver, with both normal and tangential loading, capable of modeling both load and displacement driven variations.

2. LOAD-DRIVEN ELASTIC CONTACT PROBLEM

The framework for the elastic contact solver consists of the following assumptions / limitations:

1. Contact area is small compared to dimensions of the contacting bodies, so the half-space approximation holds.
2. Only small strains and small displacements are considered.
3. The contact is dry and friction is not accounted for.

Numerical resolution of elastic contact problem relies on considering continuous distributions as piecewise constant on the elements of a mesh including the contact area. This approach allow for transforming the integral contact equation, which accepts analytical solutions only in a few cases, in a linear system of equations in pressure. Its solution can be found by numerical means; however, only fast iterative algorithms are suitable for implementation.

Only a small domain, which is expected to include the contact area and the subsurface, needs to be considered. This is an important advantage of this method over finite element analysis (FEA), where the entire bulk has to be meshed. In order to keep the

discretization error at a minimum level, a good resolution is required, especially when considering rough contact problem.

Kalker and van Randen, [5], reformulated the elastic contact problem as a problem of minimization, where the unknown contact area and pressure distribution are those who minimize the total complementary energy, under the restrictions that pressure is positive on the contact area and there is no interpenetration.

This formulation finally reduces to solving a set of equations and inequalities which have to be satisfied simultaneously. Model parameters are accompanied by subscripts which index the cell on which the parameter is bound.

The load-driven elastic contact problem model consists of the following equations and inequalities which have to be satisfied simultaneously:

$$h_{ij} = hi_{ij} + u_{ij} - \omega, (i, j) \in D \quad (1)$$

$$h_{ij} = 0, p_{ij} > 0, (i, j) \in A \quad (2)$$

$$h_{ij} > 0, p_{ij} = 0, (i, j) \in D - A \quad (3)$$

$$\Delta \sum_{(i,j) \in A} p_{ij} = W \quad (4)$$

with: h – the gap between the deformed contact surfaces; hi – the initial gap (without loading); u – the composite displacements of the contact surfaces, ω - rigid-body approach, W – the load transmitted through contact, A - contact area, D - computational domain.

The numerical formulation cannot predict singularities in the computed fields, as it employs values averaged over the elementary cell, but allows for the use of influence coefficients based methods.

The model can be solved using a modified conjugate gradient method (CGM) originally proposed by Polonsky and Keer, [7]. This algorithm has two main advantages over similar minimization methods. First, convergence is assured, as there is proof of convergence for the CGM. More, the rate of convergence is superlinear. Theory states that CGM should converge in a number of iterations equal to the number of non-nil unknowns,[8] , namely the numbers of cells in contact. In practice, a much faster convergence was observed for smooth contact geometries. Second, the algorithm allows for imposing additional restrictions in the course of CG iterations. This means the contact area is iterated during pressure correction, based on non-adhesion, Eq. (2), and non-penetration principles, Eq. (3). The force balance condition, Eq. (4), is also imposed to correct the pressure distribution. This eliminates the need for additional nested loops, which were present in most contact solvers prior to this approach.

Further tweaking of the numerical implementation involves the use of fast methods like the discrete convolution fast Fourier transform technique by Liu, Wang and Liu, [6]. This exploits the remarkable property of convolution-type products in the time-space domain to reduce to an element-wise product in the frequency domain, thus reducing computational task from $O(N^2)$ to $O(N \log N)$. However, when using spectral methods, one tacitly assumes the problem is periodic, and consequently introduces an error often referred to as the periodicity error. According to [6], this is completely avoided when using a domain extension of ratio two for every direction, together with zero padding and wrap-around order.

3. DISPLACEMENT-DRIVEN FORMULATION AND SOLUTION

A variation to the load-driven model can equally be formulated, by imposing the normal approach ω and by removing the normal load W from input. Consequently, static force Eq. (4) cannot be used to adjust pressure distribution, as load is unknown. Apparently, compared to the load-driven formulation, the number of available equations is reduced by one, while the number of unknowns is kept constant. However, the algorithm advanced by Polonsky and Keer bears a remarkable feature, namely it doesn't require normal approach as input to solve the problem. Indeed, a rigorous implementation of surface separation equation, Eq. (1), would require the rigid body displacement to be known in order to compute the residual. Yet, the following form is used in the original algorithm:

$$r_{ij} = h_{ij} + u_{ij}, (i, j) \in D \quad (5)$$

Let us assume for a moment that normal approach is known (either by problem input or by initial guess value), and residual computation is performed accordingly to Eq. (1):

$$h_{ij} = h_{ij} + u_{ij} - \omega, (i, j) \in D \quad (6)$$

In the following step, residual is adjusted by its mean on the contact area:

$$h_{ij}^* = h_{ij} - \frac{\sum_{(i,j) \in A} h_{ij}}{\aleph_0(A)} = r_{ij} - \omega - \frac{\sum_{(i,j) \in A} (r_{ij} - \omega)}{\aleph_0(A)} = r_{ij} - \frac{\sum_{(i,j) \in A} r_{ij}}{\aleph_0(A)} = r_{ij}^*, (i, j) \in D \quad (7)$$

where \aleph_0 is used to denote the cardinal number of a set, and "*" normalization with respect to mean value.

Relation (7) suggests that Eq. (5) can be used instead of rigorous form (7), yielding the same distribution of adjusted residual. Consequently, in the load-driven formulation of the elastic contact problem, normal displacement is neither needed, nor computed. However, once contact area and pressure distribution computed, rigid body approach computation from interference equation (1) is straightforward.

In the displacement driven formulation, ω is known in advance, and residual correction by its mean value is no longer needed. Therefore, Eq. (6) should be used instead of (5) in the original Polonsky algorithm.

As contact area and pressure distribution are computed in an iterative manner, initial guess values are required for both. In the first iteration, all cells of the computational domain can be considered in contact, and pressure distribution can be assumed as uniform on whole contact area.

As the load transmitted through contact is no longer known, it cannot be used to compute an initial uniform pressure. Consequently, a guess value must be adopted before starting the iterations. Secondly, nodal pressures cannot be adjusted with respect to static force equation; therefore, the corresponding instruction is removed from the algorithm.

With these modifications, the algorithm for solving numerically the displacement driven elastic contact problem can be summarized in the following steps:

1. Acquire the input: contact geometry, elastic properties of the contacting materials, normal displacement.
2. Establish the computational domain, D . For non-conforming contact problems, Hertz contact area makes a good guess value. If during pressure iterations, current

- contact area is not kept inside computational domain, namely $A^{(k)} \not\subset D$, the algorithm should be restarted with a new D .
3. Establish grid parameters, based on available computational resources. While for nominal contact geometry, a 256×256 grid should suffice, real (rough) contact samples require at least 512 grids on every direction.
 4. Choose the guess value for pressure, $p_{ij}^{(0)}$ and the imposed precision ε for the conjugate gradient iteration. According to [7], the latter should be correlated with the number of grids.
 5. Start the conjugate gradient loop. Compute surface normal displacement field as a convolution between influence coefficients matrix \mathbf{K} and current pressure $\mathbf{p}^{(k)}$, using DCFFT for computational efficiency: $\mathbf{u}^{(k)} = \mathbf{K} \otimes \mathbf{p}^{(k)}$.
 6. Compute the gap distribution, corresponding to residual in CG formulation, using Eq. (6): $h_{ij}^{(k)} = hi_{ij} + u_{ij}^{(k)} - \omega, (i, j) \in D$.
 7. Compute the descent direction $\mathbf{d}_{ij}^{(k)}$ in the CG algorithm.
 8. Compute the length of the step $\alpha^{(k)}$ to be made along minimization direction: $\mathbf{t}^{(k)} = \mathbf{K} \otimes \mathbf{d}^{(k)}, \alpha = \mathbf{h}^{(k)} \mathbf{d}^{(k)} (\mathbf{t}^{(k)} \mathbf{d}^{(k)})^{-1}$. As opposed to original algorithm, $\mathbf{t}^{(k)}$ should not be normalized by its mean value
 9. Adjust nodal pressures: $p_{ij}^{(k+1)} = p_{ij}^{(k)} + \alpha d_{ij}^{(k)}$.
 10. Impose complementarity conditions. Cells with negative pressure are excluded from current contact area, and the corresponding nodal pressures are set to zero. Cells with negative gap re-enter $A^{(k)}$, and the corresponding pressures are adjusted according to step 9.
 11. Verify convergence criterion: $|\mathbf{p}^{(k+1)} - \mathbf{p}^{(k)}| \leq \varepsilon$.

Conducted numerical simulations suggest that displacement driven formulation of elastic contact problem has the same speed of convergence compared to the load driven model.

4. PROGRAM VALIDATION

Three types of contacts for which closed form solutions were advanced are considered, and analytical data is matched against digitized distributions obtained imposing either the load (LD), or the displacement (DD) drive of elastic contact problem.

The first set of simulations is concerned with Hertz contact, with analytical solution available since 1895, [4]. Axisymmetric spherical contact between a rigid sphere and an elastic half-space is simulated. For the DD formulation, normal displacement computed according to Hertz theory is inputted to the numerical program. The predicted nodal pressures agree well with the closed form solution for pressure profile, as well as with numerical distribution obtained when imposing load drive, as depicted in Fig. 1. Dimensionless pressure is defined as ratio to hertzian pressure p_H , and dimensionless radial coordinate as ratio to Hertz contact radius a_H .

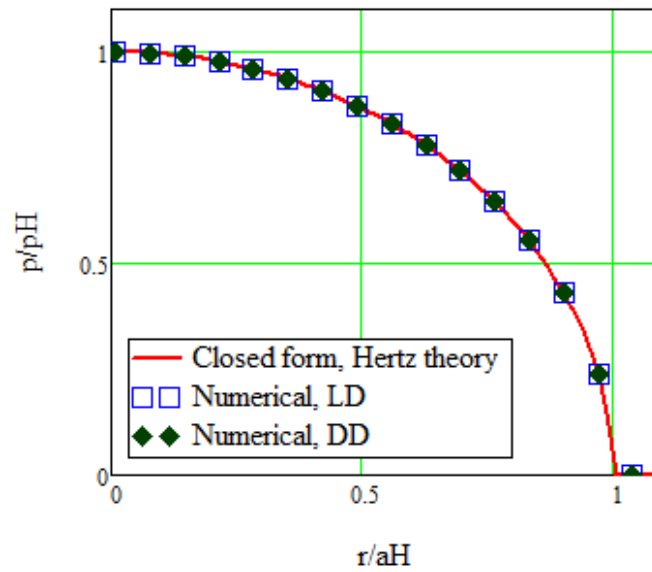


Figure 1. Pressure profiles in a radial plane, Hertz contact

To further validate the computer code, the contact between a rigid conical indenter with rounded tip and an elastic half-space was considered, Fig. 2.

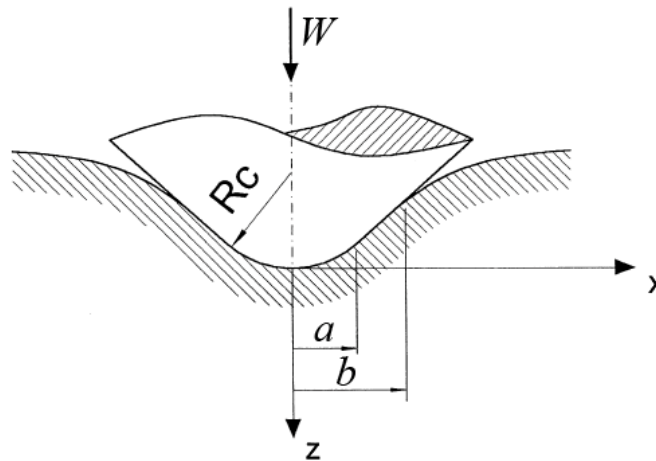


Figure 2. Contact geometry, conical indenter with rounded tip

Closed form solutions for this type of contact were advanced by Shtaerman, [9], and Ciavarella, [2]:

$$W = \frac{\theta \cdot a^2}{3\eta \cdot \cos^3 \phi_0} \cdot (4 + 3\phi_0 \cdot \cos \phi_0 - 3 \cdot \sin \phi_0 - \sin^3 \phi_0) \quad (8)$$

$$\omega = \frac{a \cdot \theta}{\cos^2 \phi_0} \cdot (1 - \sin \phi_0 + \phi_0 \cdot \cos \phi_0) \quad (9)$$

$$p(r) = p_m \cdot \frac{6 \cos \phi_0}{4 + 3\phi_0 \cdot \cos \phi_0 - 3 \cdot \sin \phi_0 - \sin^3 \phi_0} \cdot \Psi_{con} \left(\frac{r}{a} \right), 0 \leq r \leq b \quad (10)$$

where $1/R_c = \theta/a$, θ being the external cone angle, $\phi_0 = a \cos \left(\frac{a}{b} \right)$, $p_m = \frac{W}{\pi b^2}$, and

$$\Psi_{con}\left(\frac{r}{a}\right) = \begin{cases} \int_0^{a \cos \frac{r}{a}} \frac{\sin \phi \cdot d\phi}{\sqrt{1 - \frac{r^2}{a^2} \cdot \frac{1}{\cos^2 \phi}}} + \int_0^{\phi_0} \frac{\left(1 - \sin \phi + \frac{1}{2} \cdot \phi \cos \phi\right) \cdot \tan \phi \cdot d\phi}{\cos \phi \cdot \sqrt{1 - \frac{r^2}{a^2} \cdot \frac{1}{\cos^2 \phi}}}, & 0 < r < a; \\ \int_0^{\phi_0} \frac{\left(1 - \sin \phi + \frac{1}{2} \cdot \phi \cos \phi\right) \cdot \tan \phi \cdot d\phi}{\cos \phi \cdot \sqrt{1 - \frac{r^2}{a^2} \cdot \frac{1}{\cos^2 \phi}}}, & a < r \leq b. \end{cases} \quad (11)$$

In order to validate the numerical program, contact radius b , was kept at a fixed value, while varying the a/b ratio, yielding corresponding values for load and normal displacement. These values were inputted to the numerical program, and obtained pressure profiles and contact areas were matched against corresponding closed-form solutions. Hertz contact ($a = b$) was also plotted for reference. Dimensionless pressure was defined as ratio to corresponding average pressure p_m , and dimensionless radial coordinate as ratio to imposed contact area, b . A good agreement between numerical and analytical data was found, with either load, or displacement drive of the contact, as depicted in Fig. 3.

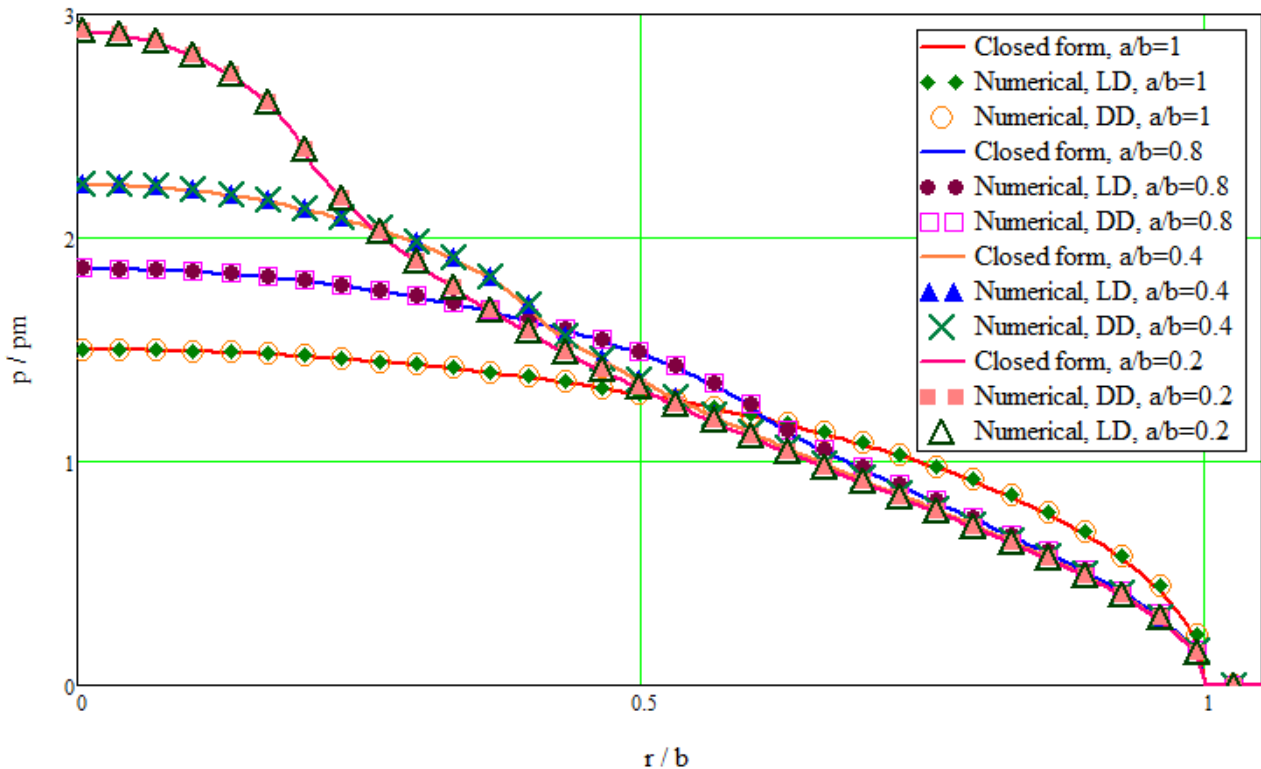


Figure 3. Pressure profiles, conical indenter with rounded tip

The case of circular flat ended punch with rounding radius, pressed against an elastic half-space, was also considered for validation purposes. It is assumed that the indenter does not penetrate too far in the half-space, so the contact plane is kept in the rounded region of the punch, as depicted in Fig. 4.

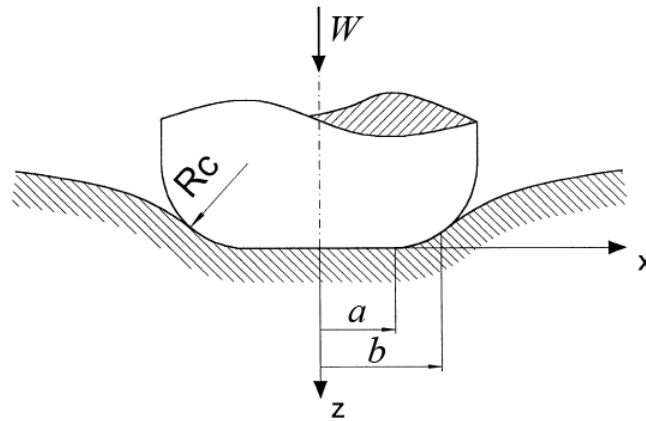


Figure 4. Contact geometry, flat end indenter with rounding radius

Closed form expressions relating contact radius b , pressure and normal displacement were advanced in [9] and in [2]:

$$W = \frac{a^3}{3\eta \cdot R_c} \cdot \frac{3 \cdot \sin \phi_0 + \sin^3 \phi_0 - 3\phi_0 \cdot \cos \phi_0}{\cos^3 \phi_0}; \quad (12)$$

$$\omega = \frac{a^2}{R_c} \cdot \frac{\tan \phi_0 - \phi_0}{\cos \phi_0}; \quad (13)$$

$$p(r) = p_m \cdot \frac{3 \cos \phi_0}{3 \cdot \sin \phi_0 + \sin^3 \phi_0 - 3\phi_0 \cdot \cos \phi_0} \cdot \Psi_{cil} \left(\frac{r}{a} \right), \quad 0 \leq r \leq b, \quad (14)$$

with $\phi_0 = a \cos \left(\frac{a}{b} \right)$, $p_m = \frac{W}{\pi b^2}$, and

$$\Psi_{cil} \left(\frac{r}{a} \right) = \begin{cases} \int_0^{\phi_0} \frac{(2 \tan \phi - \phi) \cdot \tan \phi \cdot d\phi}{\sqrt{1 - \frac{r^2}{a^2} \cdot \cos^2 \phi}}, & 0 < r < a; \\ \int_{a \cos \frac{a}{r}}^{\phi_0} \frac{(2 \tan \phi - \phi) \cdot \tan \phi \cdot d\phi}{\sqrt{1 - \frac{r^2}{a^2} \cdot \cos^2 \phi}}, & a < r \leq b. \end{cases} \quad (15)$$

The contact radius was kept at a fixed value, while varying the a/b ratio. The resulting values for load and normal approach were inputted to numerical program. A good correlation between numerical nodal pressures and analytical curves can be seen in Fig. 5. Hertz contact, corresponding to case $a = 0$, was also added for reference.

In all simulations, nodal pressures generated by the displacement-driven elastic contact algorithm match well predictions of load-driven classical formulation, and also closed form expressions from existing analytical solutions.

The number of iterations required to assess contact area and pressure distribution in displacement-driven elastic contact problem is comparable with the one for the load-driven formulation.

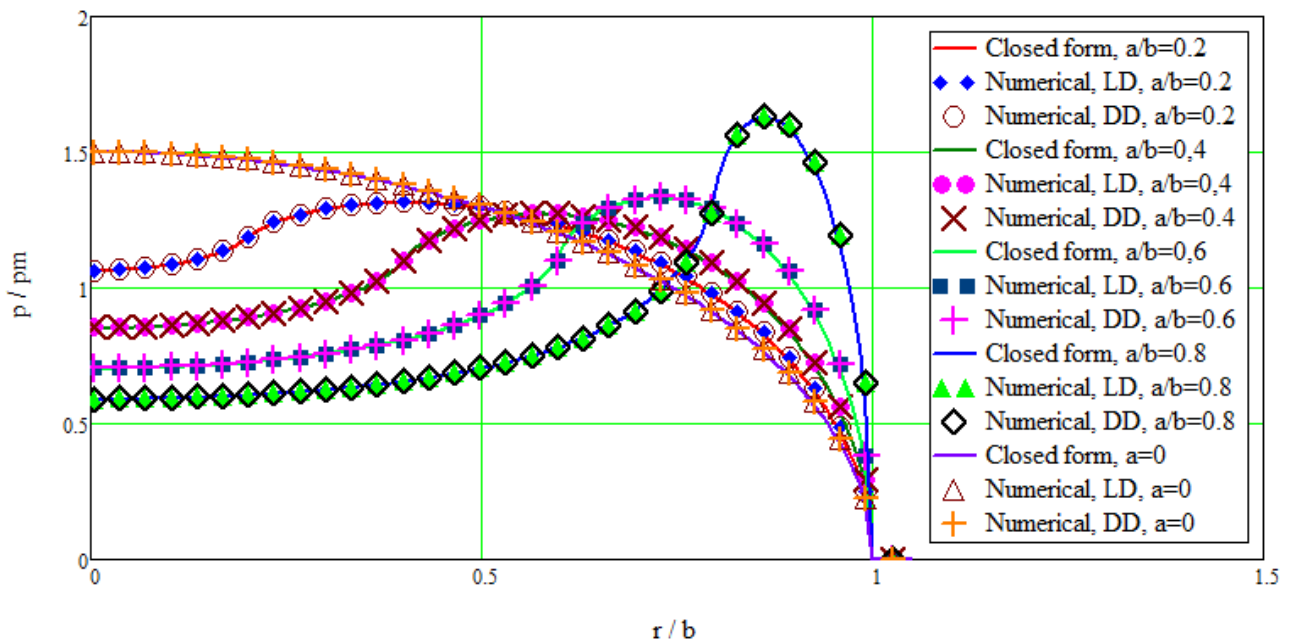


Figure 5. Pressure profiles, circular flat ended punch with rounding radius

5. CONCLUSIONS

Elastic contact problem is solved numerically by imposing a displacement driven formulation, in which the load transmitted through contact is not known, but the normal displacement is. The newly proposed algorithm is based on the rough contact solver advanced by Polonsky and Keer, [7], for load-driven contact problems.

The rigid-body approach is introduced explicitly in the residual computation, and instructions for normalization by mean value are removed. Pressure correction according to force balance equation is also detached, as normal force is unknown. However, a guess value for this is assumed when imposing initial pressure distribution. Algorithm modifications do not impair the speed of convergence.

The newly proposed algorithm is validated against analytical results for three types of conforming or concentrated contacts, and also against numerical predictions for the load-driven formulation. In all cases, a good agreement is found, giving confidence in the newly proposed algorithm.

REFERENCES

- [1] Boucly, V., Nélias, D., and Green, I., (2007), *Modeling of the Rolling and Sliding Contact Between Two Asperities*. ASME J. Tribol., 129, pp. 235 - 245.
- [2] Ciavarella, M., (1999), *Indentation by Nominally Flat or Conical Indenters with Rounded Corners*. Int. J. Solids Struct., 36, pp. 4149-4181.
- [3] Gallego, L., (2005), *Fretting et Usure des Contacts Mécaniques: Modélisation Numérique*. Ph.D. Thesis, INSA Lyon, France.
- [4] Hertz, H., (1895), *Über die Berührung fester elastischer Körper*. Gesammelte Werke, Bd. 1, Leipzig, 155-173.
- [5] Kalker, J. J., van Randen, Y. A., (1972), *A Minimum Principle for Frictionless Elastic Contact with Application to Non-Hertzian Half-Space Contact Problems*. J. Eng. Math., Vol. 6(2), pp. 193-206.
- [6] Liu, S. B., Wang, Q., and Liu, G., (2000), *A Versatile Method of Discrete Convolution and FFT (DC-FFT) for Contact Analyses*. Wear, 243 (1-2), pp. 101-111.
- [7] Polonsky, I. A., and Keer, L. M., (1999), *A Numerical Method for Solving Rough Contact Problems Based on the Multi-Level Multi-Summation and Conjugate Gradient Techniques*. Wear, 231(2), pp. 206-219.
- [8] Shewchuk, J. R., (1994), *An Introduction to the Conjugate Gradient Method Without the Agonizing Pain*. School of Computer Science, Carnegie Mellon University.
- [9] Shtaerman, I., (1949), *Contact Problems in the Theory of Elasticity*, (in Russian), Gostehizdat, Moscow.